Available online at www.sciencedirect.com

ScienceDirect

Procedia Engineering 64 (2013) 593 – 602

Procedia Engineering

www.elsevier.com/locate/procedia

International Conference On DESIGN AND MANUFACTURING, IConDM 2013

Study of effect of unbalanced forces for high speed rotor

H.K.Yadav[a*], S H Upadhyay[a] and S P Harsha[a]

[a] Mechanical & Industrial Engineering Department, Indian Institute of Technology Roorkee, Roorkee – 247 667, India

Abstract: The present paper deals with the study of dynamic behavior of unbalanced rotor along with internal radial clearance (IRC-C3) as non-linearity. Even though the perfect alignment and precision manufacturing has been done, unbalance forces cannot be eliminated completely. The dynamic behavior of a high speed unbalanced rotor has been studied for the deep groove ball bearing having the internal radial clearance of class 3. The complex mathematical model simulates nonlinear vibrations due to both nonlinear contact stiffness and damping at the contact of balls and races. The contact of rollers with races are treated as nonlinear springs with contact damping whose stiffnesses are obtained by using Hertzian elastic contact deformation theory. The explicit type numerical integration technique Runge-Kutta-Fourth-Order method is used to solve the coupled nonlinear differential equations iteratively. Various techniques like Poincare maps, orbit plots and power spectra are used to study the nature of response. The quasiperiodic behavior is a route to chaos.

Keywords: Unbalanced rotor, quasiperiodic, internal radial clearance, non linear dynamic response, chaos.

Nomenclature

k_{in}	=	Equivalent non-linear contact stiffness of the roller-inner race contact
k_{out}	=	Equivalent non-linear contact stiffness of the roller-outer race contact
$k_{in\text{-}contact}$	=	Contact stiffness of the roller-inner race contact
$k_{out\text{-}contact}$	=	Contact stiffness of the roller-outer race contact
T	=	Kinetic energy of the bearing system
V	=	Potential energy of the bearing system
m_{in}	=	Mass of the inner race, kg
m_j	=	Mass of the rolling elements, kg
m_{out}	=	Mass of the outer race, kg
m_{rotor}	=	Mass of the rotor, kg
N_b	=	Number of balls
R	=	Radius of outer race, mm
r	=	Radius of inner race, mm
c	=	Contact damping
c_{in}	=	Equivalent contact damping factor of roller-inner race contact
c_{out}	=	Equivalent contact damping factor of roller-outer race contact
d	=	Ball diameter, mm
D	=	Pitch diameter of bearing, mm
F_{di}	=	Total damping contact force of the ith ball, N

* Corresponding author. *E-mail address:* himanshukyadav2@gmail.com

doi:10.1016/j.proeng.2013.09.134

$F_{d\text{-}in}$	=	Ball-inner race contact damping force, N
$F_{d\text{-}out}$	=	Ball-outer race contact damping force, N
Q	=	Contact force, N
R	=	Radius of outer race, mm
r	=	Radius of inner race, mm
W	=	Radial preload, N
VC	=	Varying compliance frequency, Hz
FTF	=	Cage Frequency, Hz
X	=	Rotational Frequency due to unbalanced weight, Hz
FFT	=	Fast Fourier Transformations
Greek symbols		
δ_{in+}	=	Contact deformation of the roller-inner race, μm
δ_{out+}	=	Contact deformation of the roller-outer race, μm
γ_0	=	Internal radial clearance, μm
$\sum\rho$	=	Sum of curvature of the contacting bodies
$(\dot{\phi})_{in}$	=	Angular velocity of inner race, rad/s
$(\dot{\phi})_{out}$	=	Angular velocity of outer race, rad/s
β	=	Constant angular separation between rolling elements, deg
χ_j	=	Radial position of jth rolling element from center of inner race, mm
ρ_j	=	Radial position of jth rolling element from center of outer race, mm
ρ_r	=	Radius of each rolling element, mm

1. Introduction:

Ball bearing is one of the vital and crucial elements of small to large rotating machinery. It has very complicated dynamic behavior due to number of rolling element except the fixed outer race or inner race. Not only that, but its motion behavior is very sensitive to initial condition also. Further, each shaft is supported at the two ends by two ball bearings and different type of rotor like gear or pulley is mounted on that shaft. Now, this gear or pulley will create the unbalance forces, because the centre of mass of rotor and shaft is not generally coincided. This unbalanced forces is changed continuously with change in the speed of rotor and changing the dynamic behavior of the whole system continuously. So, in the present paper the authors' main intense is to study the effect of unbalance force on the dynamic behavior of the unbalanced rotor system.

Harsha [1] is the first who has study the effect of unbalanced forces for cylindrical rolling element bearing which has 8 no of roller. It was concluded that route to chaos is intermittence mechanism due to periodic doubling behavior. While Tiwari et al [2] has been studied the effect of unbalanced rotor supported by deep groove ball bearing SKF 6002 having 9 no of balls. The study was conducted by numerically and experimentally both. The conclusion was that the chaotic behavior has been occurred due to intermittent mechanism through periodic doubling behavior. It was also concluded that frequency spectra displayed multiples of 1X and VC and the linear combination of the two frequencies.

Upadhyay et al [3] has been studied the effect of unbalanced rotor in more detail along with the effect of internal radial clearance as nonlinearity. Finally, the different region of periodic, quasiperiodic and chaotic has been identified. Sunnersjo [4] studied the varying compliance vibrations theoretically and experimentally, taking inertia and damping forces into account. Fukata et al. [5] first took up the study of varying compliance vibrations and the nonlinear dynamic response for the ball bearing supporting a balanced horizontal rotor with a constant vertical forces. It is a more detailed analysis compared with Sunnersjo's [4] works as regimes of super-harmonic, sub-harmonic and chaotic behavior are discovered.

The varying compliance effect was studied theoretically by Perret [6] considering a deep groove ball bearing with the elastic deformation between race and balls modeled by the Hertzian theory and no bending of races. Meldau [7] studied theoretically the two-dimensional motion of shaft center. Both Perret [6] and Meldau [7] performed a quasi-static analysis since inertia and damping forces were not taken into account. Mevel and Guyader [8] have developed a theoretical model of

a ball bearing supporting a balanced horizontal rigid rotor, with a constant vertical radial force. This is similar to the work done by Fukata et al. [5], but more results have been reported for parametric studies undertaken and routes to chaos traced out. Chaos in this model of bearing has been reported to come out of the sub-harmonic route and the quasi-periodic route. Datta and Farhang [9] developed a nonlinear model for structural vibration in the rolling bearings by considering the stiffness of the individual region where the elements contact each other but in this model distributed defects are not considered. Tiwari et al. [10] has studied the effect of radial internal clearance_ the appearance of sub-harmonics and Hopf bifurcation is seen theoretically where as the shift in the peak response is also observed experimentally.

Harsha et al. [11] analyzed the nonlinear behavior of a high speed horizontal balanced rotor supported by a ball bearing. The conclusion of this work shows that the most severe vibrations occur when the varying compliance frequency (VC) and its harmonics coincide with natural frequency. Harsha [12] has studied the effects of radial internal clearance and rotor speed. The appearance of periodic, sub-harmonic, chaotic and Hopf bifurcation is seen theoretically. But Harsha considered only nonlinear stiffness. Harsha [13] studied the effects of radial internal clearance for balanced rotor. The appearance of periodic, sub-harmonic, chaotic and Hopf bifurcation is seen theoretically. But he has considered only nonlinear stiffness. Harsha [14] has studied the effects of rotor speed with geometrical imperfections. The results are from a large number of numerical integrations and are mainly presented in the form of Poincare maps and frequency spectra.

Cao et al. [15] has developed the comprehensive mathematical model for the spherical roller bearing. This paper represents that the larger the radial clearance, the higher the modal density; and the higher the response at the roller passing frequency and its super harmonics. But overall the benefit of smaller radial clearance is limited in reducing the displacements of inner race. Also, it has been shown by Ghafari et al [16] that the bearing having the clearance more than 4.5μm has more than one equilibrium point noted as strange attractor. The system vibrates around these strange attractors randomly. It has been reported that bearing having clearance more than 12μm has chaotic nature at 1000RPM onwards

So, after detailed literature survey, the authors have decided to study the unbalanced rotor along with the internal radial clearance as nonlinearity. The study has been done for the deep groove ball bearing having 9 no. of balls and shaft diameter is 25mm. The bearing has internal radial clearance of class C3 (13μm) and unbalanced forces is taken as 10% of radial load (W).

2. Problem formulation:

A schematic diagram of rolling element bearing is shown in Fig. 1. For investigating the structural vibration characteristics of rolling element bearing, a model of bearing assembly can be considered as a spring mass damper system. Elastic deformation between races and balls gives a non-linear force deformation relation, which is obtained by Hertzian theory. In the mathematical modeling, the rolling element bearing is considered as spring mass damper system and rolling elements act as non-linear contact spring as shown in Fig.2.

Since, the Hertzian forces arise only when there is contact deformation, the springs are required to act only in compression. In other words, the respective spring force comes into play when the instantaneous spring length is shorter than its unstressed length, otherwise the separation between balls and the races takes place and the resultant force is set to zero. The excitation is because of the varying compliance vibrations of the bearing which arise because of the geometric and elastic characteristics of the bearing assembly varying according to the cage position

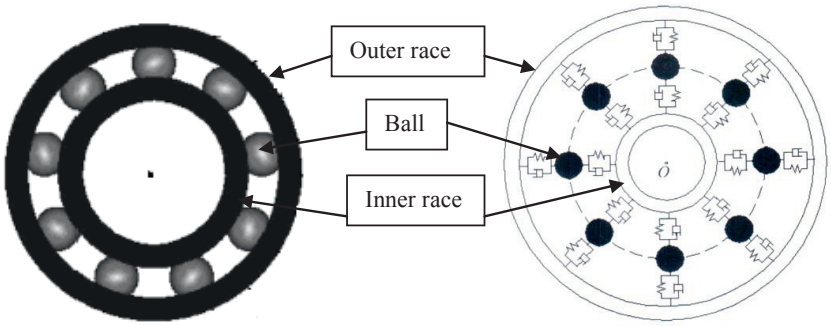

Fig.1. The flexibiltiy of the rolling contacts in a rolling element bearing is represented by non-linear spring and non-linear damper

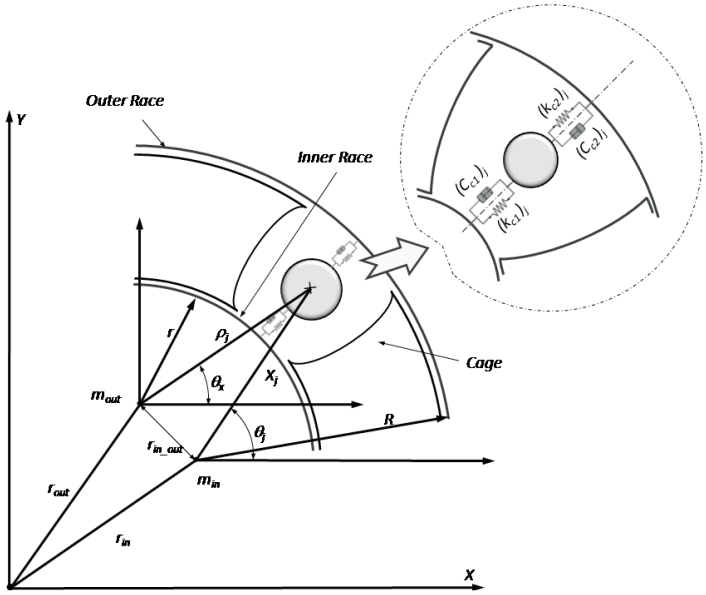

Fig. 2. Mass-spring-damper of rolling element bearing

.

The equations of motion that describe the dynamic behavior of the complete model can be derived by using Lagrange's equation for a set of independent generalized coordinates, as:

$$\frac{d}{dt}\frac{\partial T}{\partial\{\dot{p}\}}-\frac{\partial T}{\partial\{p\}}+\frac{\partial V}{\partial\{p\}}+\frac{\partial P_d}{\partial\{\dot{p}\}}=\{f\} \tag{2}$$

where T, V, p and f are kinetic energy, potential energy, vector with generalized degree-of-freedom (DOF) coordinate and vector with generalized contact forces respectively and P_d represent the dissipation energy due to damping. The kinetic and potential energies can be subdivided into the contributions from the various components i.e. from the rolling elements, the inner race, the outer race and the rotor.

The kinetic energy and potential energy contributed by the inner race, outer race, balls, rotor and springs, can be differentiated with respect to the generalized coordinates ρ_j ($j = 1,2,\ldots\ldots, N_b$), x_{in}, and y_{in} to obtain the equations of motion. For the generalized coordinates ρ_j, where $j = 1,2,\ldots\ldots, N_b$, the equations are:

$$\begin{aligned}
&\ddot{\rho}_j+g\sin\theta_j+\rho_j\dot{\theta}^2-\frac{1}{m_j}\left(k_{in_contact}\right)\left[\delta_{in}\right]_+^{3/2}\frac{\partial\chi_j}{\partial\rho_j}+\frac{1}{m_j}\left(k_{out_contact}\right)\left[\delta_{out}\right]_+^{3/2}\\
&+\frac{1}{2m_j}\frac{\partial\left[\left(k_{in_contact}\right)\left(\left[\delta_{in}\right]_+^{1/2}\right)\right]}{\partial\rho_j}\left[\delta_{in}\right]_+^2+\frac{1}{2m_j}\frac{\partial\left[\left(k_{out_contact}\right)\left(\left[\delta_{out}\right]_+^{1/2}\right)\right]}{\partial\rho_j}\left[\delta_{out}\right]_+^2\\
&+\frac{3}{2m_j}\sum_{j=1}^{N_{r.e}}\left\{C_{in}\left(K_{in_contact}\right)\delta_{in_+}^{3/2}\left(-\chi_j\right)^q\frac{\partial\dot{\chi}_j}{\partial\dot{\rho}_j}\right\}\\
&+\frac{3}{2m_j}\sum_{j=1}^{N_{r.e}}C_{out}\left(K_{out_contact}\right)\delta_{out_+}^{3/2}\left(-\dot{\rho}_j\right)^q=0 \qquad j=1,2,\ldots\ldots,N_b
\end{aligned} \tag{3}$$

For the generalized coordinate x_{in} the equation is:

$$\ddot{x}_{in} - \frac{1}{m_{rotation}} \sum_{j=1}^{r.e} \left(k_{in\_contact}\right) \left[\delta_{in}\right]_{+}^{3/2} \frac{\partial \chi_j}{\partial x_{in}} + \frac{3}{2 m_{rotation}} \sum_{j=1}^{N_{r.e}} \left\{ C_{in} \left(K_{in\_contact}\right) \delta_{in+}^{3/2} \left(-\dot{\chi}_j\right)^q \frac{\partial \dot{\chi}_j}{\partial \dot{x}_{in}} \right\} = \frac{F_u \sin(\omega_s t)}{m_{rotation}} \tag{4}$$

For the generalized coordinate y_{in} the equation is:

$$\ddot{y}_{in} + g - \frac{1}{m_{rotation}} \sum_{j=1}^{N_b} \left(k_{in\_contact}\right) \left[\delta_{in}\right]_{+}^{3/2} \frac{\partial \chi_j}{\partial y_{in}} + \frac{3}{2 m_{rotation}} \sum_{j=1}^{N_{r.e}} \left\{ C_{in} \left(K_{in\_contact}\right) \delta_{in+}^{3/2} \left(-\dot{\chi}_j\right)^q \frac{\partial \dot{\chi}_j}{\partial \dot{y}_{in}} \right\} = \frac{\left(W + F_u \cos(\omega_s t)\right)}{m_{rotation}} \tag{5}$$

where, $m_{rotation} = \left(m_{inner} + m_{rotor}\right)$

This is a system of $(N_b + 2)$ second order, non-linear differential equations. There is no external radial force is allowed to act on the bearing system and no external mass is attached to the outer race. The "+" sign as subscript in these equations signifies that if the expression inside the bracket is greater than zero, then the rolling element at angular location θ_j is loaded giving rise to restoring force and if the expression inside bracket is negative or zero, then the rolling element is not in the load zone, and restoring force is set to zero. For the balanced rotor condition, the unbalanced rotor force (F_u) is set to be zero.

In the present paper, the authors have written the equation of motion directly. The derivation of the equation of motion has been explained in detail in the reference Upadhyay et al [17].

3. Numerical solution of coupled non linear ODE equations:

The coupled non-linear second order differential Eq.s (3 to 5) is solved by numerical integration technique which is a time domain approach. The non-analytic nature of the stiffness term renders the system equations difficult for analytical solution.

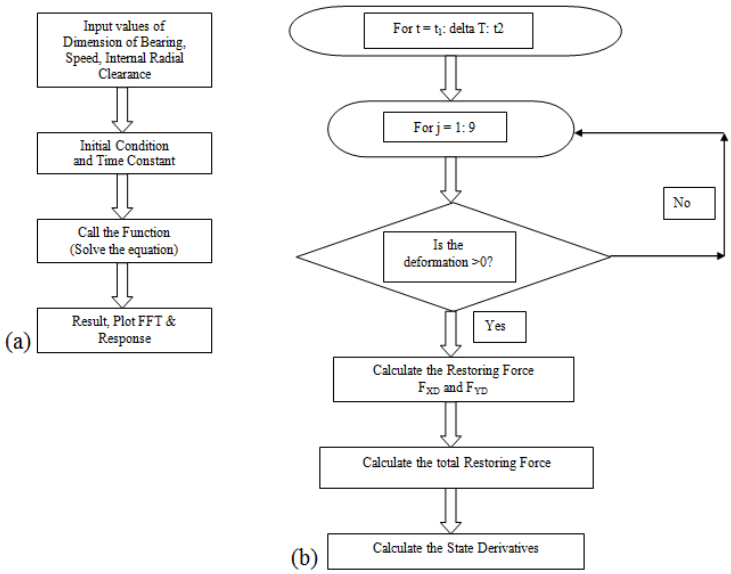

Fig. 3. Flow chart of (a) main program (b) call function

4. Results and discussion:

To get the satisfactory post transient steady state condition, numerical simulation is run for 2sec. To save the computational time, artificial damping, c =50N-s/m is used. In the present study, DGB bearing SKF 6205, class 3 type is used, in which internal radial clearance is 13μm.The other geometrical and physical properties of bearing is listed in Table 1. All sharp peaks of modulated frequencies present in all FFT plots are listed in Table 2.

In the present paper, weight of balanced rigid rotor (50N) is taken as constant radial load (W) and different types of nonlinear behavior is identified for the speed range of 1000RPM to 10,000RPM. Unbalanced weight is taken as 10% of weight of rigid rotor. Results of simulation of this study like Poincare plot and power spectrum for horizontal displacement has been shown in Fig. 4 and Fig. 5. As the speed is changing, the dynamical behavior of the system is changed. From this study it has been observed that at 4000RPM, 5000RPM, 6000RPM, 9000RPM and 10000RPM there is an occurrence of chaos through the quasiperiodic routes to chaos.

Fig. 4 (a) & Fig. 4 (b) shows the Power spectrum and Poincare map for horizontal motion at 1000RPM, respectively. Peaks of variance compliance frequency (VC) with its multiples and rotational frequency (X) are present in FFT plot (Fig 4 (a)). Also, it can be observed that, the different peak of modulated frequency of these two fundamental frequencies present in Fig. 4 (a). All these different peaks are listed in Table 2. So, in this case it is possible to represent all frequency as a linear

Table 1 Geometrical and physical properties of the DGB bearing SKF 6205

Bearing specification	SKF 6205
Mass of the rotor (m_r)	5kg
Radius of inner race with point of contact with the rolling element (r)	15.56mm
Radius of outer race with point of contact with the rolling element (R)	23.5mm
Radius of each rolling element (ρ_r)	3.965mm
Radial load (W)	50N
Unbalanced weight (F_u)	10% of W
Outside diameter	52 mm
Number of rolling elements (N_b)	9
Angular separation between elements ($\beta = 2\pi / N_b$)	40 deg
Bearing clearance (μm)	13

Table 2 List of major and minor peaks for horizontal displacement

RPM	Max. Peak	Other peaks
1000	X	VC,2VC,3VC,4VC,5VC+X, 4VC+X,VC-X,VC+X,X+FTF
2000	X	2X,VC,2VC, VC-X,VC+X,2VC+X,2VC-X,2VC-X+2FTF,
3000	X	2X,VC,2VC,VC-X,VC+X, 2VC-X,2VC+X ,2VC+2X, 2VC-2X,VC-2X OR X+FTF,VC+2X, X-FTF
4000	VC	X,2X,2VC,VC-X,VC+X,2VC+X,2VC-X,VC+FTF
5000	X	FTF,VC,2VC, VC-X,VC+X, VC-2X , VC+2X,VC-X-FTF,VC+FTF, 2VC-X,
6000	X	FTF,VC,VC-X,VC+X, VC-X+FTF,
7000	X	2X,VC,VC-X,VC+X,VC+2X,VC-2X OR 2X-FTF, X-FTF OR VC-3X
8000	X	2X,VC, FTF, VC-X,VC+X,VC+2X,VC-2X,
9000	X	VC,2X, VC-X, VC-2X,VC-3X,X+1.5VC
10,000	X	VC,2X, VC-X, VC-2X,X+FTF

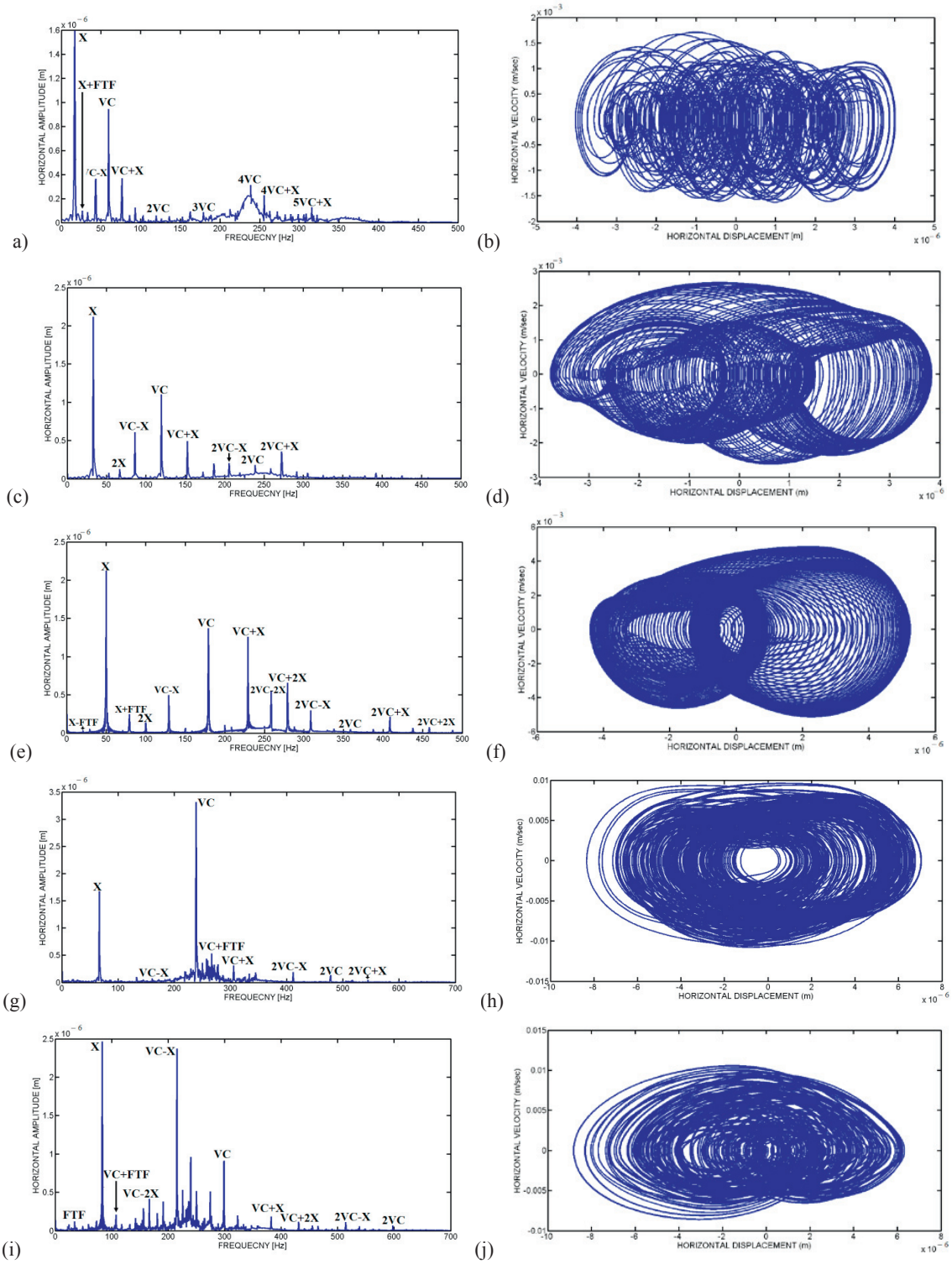

Fig.. 4. FFT plots at (a) 1000 RPM (c) 2000 RPM (e) 3000 RPM (g) 4000 RPM (i) 5000RPM and Poincare plot at (b) 1000 RPM (d) 2000 RPM (f) 3000 RPM (h) 4000 RPM (j) 5000RPM

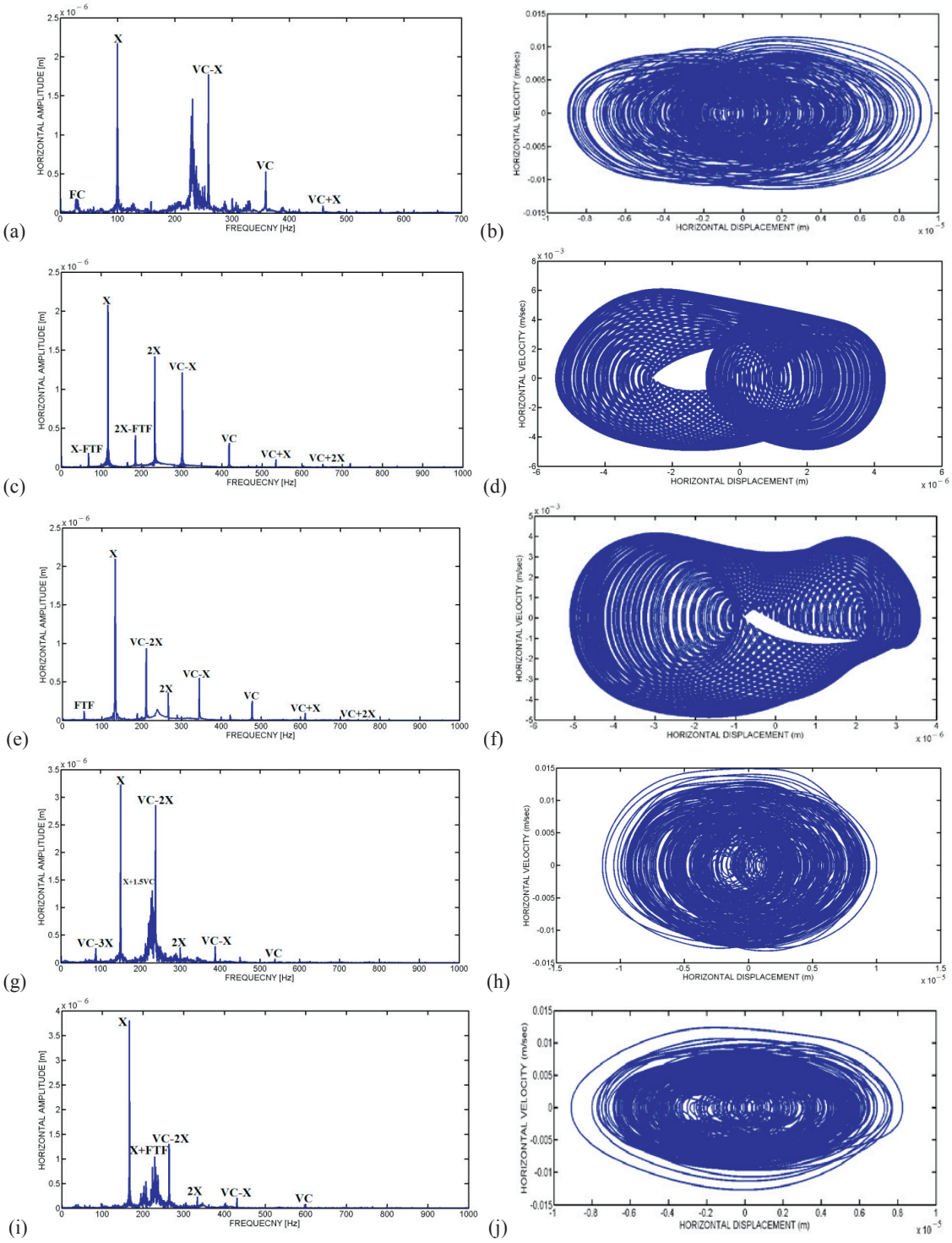

Fig.. 5. FFT plots at (a) 6000 RPM (c) 7000 RPM (e) 8000 RPM (g) 9000 RPM (i) 10,000RPM and Poincare plot at (b) 6000 RPM (d) 7000 RPM (f) 8000 RPM (h) 9000 RPM (j) 10,000RPM

combination of two fundamental frequencies VC and X. Also, ratio of these two frequencies is incommensurate. So, it can be inferred that the motion is quasiperiodic. But, it is unstable quasiperiodic motion because the Poincare map has dense orbit instead of net type structure as shown in Fig. 5 (b). So, at 1000 RPM the behavior of motion is unstable quasiperiodic type of second order due to presence of two fundamental frequencies.

Similarly for 2000RPM, in power spectra two fundamental frequency VC and X along with their superharmonics can be observed as shown in Fig. 4 (c). The major peak is of rotational frequency (X). In addition to that, proper net structures of Poincare map, as shown in Fig. 4 (d), indicates the stable quasiperiodic motion. Poincare maps at 2000 RPM have more ordered net structure compared to the same at 1000RPM. So, that is the reason to say that, the motion at 2000RPM is quasiperiodic stable. And, it is of the second order type because the presences of two fundamental frequencies VC and X in FFT plot.

In case of 3000RPM, the Poincare map has net structure which is shown in Fig. 4. (f). Also, sharp peak of two fundamental frequency X and VC can be observed in Fig.4.(e). In addition to that, sharp peak of modulated frequency of these two fundamental frequencies is also present in FFT plot as shown in Fig.4 (e). So, the motion at 2000RPM is quasiperiodic stable and it is of the second order type because the presences of two fundamental frequencies VC and X in FFT plot.

Now, at the 4000RPM the motion is chaotic which can be predicted by the dense orbit at the centre in the Poincare map as shown in Fig. 4 (h). Two fundamental frequencies X and VC are present in FFT plot as shown in Fig.4 (g). Also, dense power spectrum can be observed around the peak VC – FTF, Which is also indicating the chaotic motion. This chaotic motion is still continued at 5000RPM which is concluded from the dense centered orbit in the Poincare map as shown in Fig. 4 (j). Further, in Fig. 4 (i), there is a two major peak X and VC – X, and around VC –X there is a continuous broad band of frequencies. Apart from two fundamental frequencies VC and X, a very small peak of FTF can be seen in Fig. 4 (i).

At 6000 RPM, major peak are X and VC-X and around it little bit continuous broad band is present as shown in Fig. 5 (a). Dense orbit at the centre in case of Poincare map as shown in Fig. 5 (b) shows chaotic motion. A very small individual peak of cage frequency FTF is present as shown in Fig. 5 (a). Now, perfectly net type structure in Fig. 5(d) infers the quasiperiodic motion at 7000RPM. Also, two fundamental frequency and their modulated frequencies are present in both FFT plots as shown in Fig. 5 (a). Also, only sharp peaks are present in the FFT plot. This indicates that chaotic motion is over and the system has second order quasiperiodic motion. At 8000RPM, the motion is third order type quasiperiodic which can be concluded due to the presence of sharp peaks of three fundamental frequencies VC, X and FTF. Further, a complete ordered net structure as shown in Fig. 5 (f) represents the same fact that the motion is quasiperiodic.

Now, at 9000RPM both the FFT plots have continuous broad band around VC-2X as shown in Fig. 5 (g) which represents the chaotic motion. Further Poincare map has very dense orbit at centre as shown in Fig. 5 (h). So, it is obvious that at 9000 RPM motion is chaotic type. Also, peaks of modulated frequencies like VC-2X, VC-X, and VC-3X can be observed. Now, the chaotic motion is continued at 10,000RPM also which can be concluded from very dense orbit at the centre of Poincare map as shown in Fig. 5 (j). In Fig. 5 (i), major peaks are X and VC-2X, and between these two continuous power spectra is also present which also represents chaotic motion.

5. Conclusion

Based on result and discussion, following points can be concluded.

- The system has chaotic nature at 4000RPM, 5000RPM, 6000RPM, 9000RPM, and 10,000RPM through quasiperiodic route to chaos. At 1000RPM, the system has unstable quasiperiodic behavior of second order type. While at 2000RPM, 3000RPM and 7000RPM, the system behaves as stable quasiperiodic of second order type. And at 8000RPM, the dynamic nature of the system is 3rd order quasiperiodic motion.
- In power spectrum, presence of rotational frequency X is due to the unbalanced forces.
- As compared to balanced rotor, in case of unbalanced rotor presence of superharmonics and subharmonics in power spectra are less.
- In case of balanced rotor the system has multiperiodic behavior and a route to chaos is almost subharmonics of VC, while in case of unbalanced rotor, a route to chaos is quasiperiodic unstable motion.
- In case of quasiperiodic stable motion, the Poincare map has perfectly ordered “net” structure.

- The system has more variation in vertical direction compared to horizontal direction which is also reported by Harsha [1], Upadhyay [3], Cao [15], Tiwari [10] and Fukata [5].
- Magnitude of vertical displacement is less compared to horizontal displacement which is also reported by Harsha [1], Upadhyay [3], Cao [15], Tiwari [10] and Fukata [5].

References:

[1] Harsha, S., 2005b. Non-linear dynamic analysis of an unbalanced rotor supported by roller bearings, Chaos, Solitons & Fractals 26, p.47.
[2] Tiwari, M., Gupta, K., Prakash, O., 2000a. Dynamic Response of an Unbalanced Rotor Supported on Ball Bearings" Journal of Sound and Vibration, 238(5), p. 757.
[3] Upadhyay, S., Harsha, S., Jain, S. 2010. Analysis of Nonlinear Phenomena in High Speed Ball Bearings due to Radial Clearance and Unbalanced Rotor Effects, Journal of Vibration and Control, 16(1), p.65.
[4] Sunnersjo, C., 1978. Varying compliance vibrations of rolling bearings, Journal of Sound and Vibration 58, p.363.
[5] Fukata, S., Gad, E., Kondou, T,Ayabe, T,.Tamura, H., 1985. On the radial vibrations of ball bearings (computer simulation), Bulletin of the Japan Society of Mechanical Engineers 28, p.899.
[6] Perret, H., 1950. Elastiche Spielschwingungen Konstant Belaster Walzlger, Werstatt und Betrieb 3, p.354.
[7] Meldau, E., 1951 Die Bewegung der Achse von Walzlagern bei geringen Drehzahlen, Werkstadt und Betreib 7, p.308.
[8] Mevel, B., Guyader, J., 1993. Routes to Chaos in Ball Bearings, Journal of Sound and Vibration 162, p. 471.
[9] Datta, J.,Farhang, K., 1997. A nonlinear model for structural vibrations in rolling element bearings: Part I – derivation of governing equations, ASME Journal of Tribology 119, p.126.
[10] Tiwari, M., Prakash,O.,Gupta, K., 2000. Effect of radial internal clearance of a ball bearing on the dynamics of a balanced, horizontal rotor, Journal of Sound and Vibration 238(5), p. 723.
[11] Harsha, S., Sandeep, K., Prakash, R., 2003. The effect of speed of balanced rotor on nonlinear vibrations associated with ball bearings, International Journal of Mechanical Sciences 47(4), p. 225.
[12] Harsha, S., 2005a. Non-linear dynamic response of a balanced rotor supported on rolling element bearings, Mechanical Systems and Signal Processing 19, p.551.
[13] Harsha, S., 2006a. Non-linear dynamic responses of a balanced rotor supported by rolling element bearings due to radial internal clearance effect, Mechanism and Machine Theory 41, p.688.
[14] Harsha, S., 2006b.Non-linear dynamic analysis of high speed rotor supported by rolling element bearings, Journal of Sound and Vibration 290, p.65.
[15] Cao, M., Xiao, A., 2008. A Comprehensive Dynamic Model of Double-Row Spherical Roller Bearing—Model Development And Case Studies on Surface Defects, Preloads, and Radial Clearance, Mechanical Systems and Signal Processing, 22, p.467–489.
[16] Ghafari, S., Abdel-Rahman, E., Golnaraghi, F., Ismail, F., 2010. Vibrations of Balanced Fault-free Bearings, Journal of Sound and Vibration, 329, p.1332.
[17] Upadhyay, S., Jain, S., Harsha, S., 2009. Nonlinear Vibration Signature Analysis of High Speed Rotating Shaft due to Ball Size Variations and Varying Number of Balls, Proceedings of the Institution of Mechanical Engineers, Part K: Journal of Multi-body Dynamics (IMechE), 223, p.83.